Core Excitation Spectroscopy of Stable Cyclic Diaminocarbenes, -silylenes, and -germylenes

John F. Lehmann,[†] Stephen G. Urquhart,[‡] Laura E. Ennis,[†] Adam P. Hitchcock,*[,†] Ken Hatano,[§] Shilpi Gupta,[§] and Michael K. Denk[§]

Department of Chemistry, McMaster University, Hamilton, Ontario, Canada L8S 4M1, Department of Physics, North Carolina State University, Raleigh, North Carolina 27696-7518, and Department of Chemistry, University of Toronto, Mississauga, Ontario, Canada L5L 1C6

Received October 28, 1998

A number of *tert*-butyl-substituted, cyclic, saturated and unsaturated diaminocarbene, diaminosilylene, and diaminogermylene compounds were investigated using inner shell electron energy loss spectroscopy (ISEELS) and ab initio calculations. These compounds, each of which contains a divalent group 14 element (C, Si, Ge), are of particular interest since they are stable indefinitely, and thus, they are readily accessible for detailed spectroscopic analysis. The C 1s and N 1s spectra of the hydrogenated tetravalent analogues of the saturated carbene, of di-*tert*-butyldiazabutadiene, and of di-*tert*-butyldiazabutane were also obtained to assist with spectral interpretation. Our analysis shows that there is significant π-allyl delocalization over the N−E^{II}−N fragment in all three species. Further, in the unsaturated species there is additional aromatic delocalization. Both theory and experiment indicate that the divalent center of the carbene is qualitatively different from that in the germylenes or silylenes.

I. Introduction

Carbenes have long been known to be highly reactive species, historically observable only as intermediates or in cryogenic matrixes. The concept that carbenes might play a significant role as reactive intermediates dates back to the early investigations of Hine, who deduced from kinetic data that Cl_2C: was an intermediate in the base-catalyzed hydrolysis of chloroform.[1] Methylene, H_2C:, was subsequently the subject of the now classic spectroscopic studies of Herzberg et al.[2] Since then many carbenes have been isolated in frozen matrixes and investigated spectroscopically.[3] The organometallic chemistry of carbenes was initiated with the synthesis of stable carbene complexes by Fischer and Maasböl.[4] In 1964, it was discovered that several carbon−metal double bonds are in equilibrium to a small extent with the divalent carbene species when solvated.[4] In 1960−1961, Wanzlick proposed that enetetramines can dissociate into diaminocarbenes but was unable to present unambiguous proof for the presence of free carbenes.[5] The high stability of diaminocarbenes was demonstrated in 1991, when Arduengo described the synthesis and structure of 1,3-diadamantylimidazol-2-ylidene, the first unambiguously stable carbene.[6] Despite being highly air and moisture sensitive, Arduengo's carbene is stable up to 240 °C.

There are several reasons for this remarkable stability. First, the large electronegativity of nitrogen stabilizes the lone pair on the carbon center in the plane of the ring through an inductive σ-effect.[7] Second, the unoccupied carbon(II) orbital can be stabilized by mesomeric interaction with the nitrogen lone pairs. This provides about 70 kcal/mol of stabilization. A further 26 kcal/mol of stabilization is predicted to be associated with an overall $4n + 2$ aromatic Hückel configuration in the unsaturated ring.[8] The planar geometry and the proton NMR spectrum, which exhibits strongly deshielded protons at 6.91 ppm,[6] both strongly support the proposed aromatic nature of the heterocycle. Bulky substituents bound to the nitrogen centers have been shown conclusively to play a vital role in the stability of isolatable carbenes[9] and are likely requirements for the silylene and germylene analogues as well. In the

* To whom correspondence should be addressed. E-mail: aph@mcmaster.ca.
[†] McMaster University.
[‡] North Carolina State University.
[§] University of Toronto.

(1) Hine, J. *J. Am. Chem. Soc.* **1950**, *72*, 2438. Hine, J.; Dowell, A. M. *J. Am. Chem. Soc.* **1954**, *76*, 2688. Hine, J.; Dowell, A. M.; Singley, J. E. *J. Am. Chem. Soc.* **1956**, *78*, 749.
(2) Herzberg, G. *Proc. R. Soc. London, Ser. A* **1961**, *A262*, 291. Herzberg, G.; Johns, J. W. C. *Proc. R. Soc. London, Ser. A* **1964**, *A295*, 207. Herzberg, G. Nobel Prize Lecture. *Angew. Chem.* **1972**, *84*, 1126.
(3) Marchand, A. P.; Brookhart, N. M. *Chem. Rev.* **1973**, *73*, 431. Stang, P. J. *Chem. Rev.* **1978**, *78*, 383. Sander, W.; Bucher, G.; Wierlacher, S. *Chem. Rev.* **1993**, *93*, 1583.
(4) Fischer, E. O.; Maasböl A. *Angew. Chem., Int. Ed. Engl.* **1964**, *4*, 580. Fischer, E. O. In *Advances in Metal Carbene Chemistry*; Kluwer: Dordrecht, The Netherlands, 1989; pp 1−9.
(5) (a) Wanzlick, H.-W.; Schikora, E. *Angew. Chem.* **1960**, *72*, 494. (b) Wanzlick, H.-W.; Schikora, E. *Chem. Ber.* **1961**, *94*, 2389. (c) Wanzlick, H.-W.; Kleiner, H.-J. *Angew. Chem.* **1961**, *73*, 493. (d) Wanzlick, H.-W. *Angew. Chem.* **1962**, *74*, 129; Wanzlick, H.-W. *Angew. Chem., Int. Ed. Engl.* **1962**, *1*, 75. (e) Wanzlick, H.-W.; Ahrens, H. *Chem. Ber.* **1964**, *97*, 2447. (f) Wanzlick, H.-W.; Lachmann, B.; Schikora, E. *Chem. Ber.* **1965**, *98*, 3170. (g) Wanzlick, H.-W.; Schönherr, H. J. *Angew. Chem.* **1968**, *80*, 153; *Angew. Chem., Int. Ed. Engl.* **1968**, *7*, 141.
(6) Arduengo, A. J., III; Harlow, R. L.; Kline, M. *J. Am. Chem. Soc.* **1991**, *113*, 361.
(7) Cioslowski, J. *Int. J. Quantum Chem.* **1993**, *27*, 309.
(8) Herrmann, W. A.; Köcher, C. *Angew. Chem., Int. Ed. Engl.* **1997**, *36*, 2162.
(9) Denk, M. K.; Thadani, A.; Hatano, K.; Lough, A. J. *Angew. Chem., Int. Ed. Engl.* **1997**, *36*, 2607.

10.1021/om980882z CCC: $18.00
Publication on Web 04/14/1999

case of the CC-saturated carbenes, the carbene is stable only for R = ^{t}Bu and larger. For R = ^{i}Pr, Et, Me rapid dimerization to the enetetramines precludes the isolation of the diaminocarbene.[9] This is in obvious contrast to the CC-unsaturated carbenes, which can be isolated as stable species even for R = methyl.[9]

In recent years, a significant amount of research has been directed toward the isolation of heterocycles which contain divalent silicon or germanium centers. Stable carbenes, silylenes, and germylenes are valuable new building blocks for the synthetic chemistry of the respective elements. The high volatility of these compounds allows their use as CVD precursors. The germanium compound has already been shown to be an excellent CVD precursor for the deposition of electronic grade germanium thin films.[10,11] Characterization of these compounds[12] is therefore of both academic and potentially industrial interest.

The importance of aromatic π-delocalization was supported by ab initio calculations, NMR data, and PES data for the silylene and germylene.[11] For the carbene, the extent of aromatic delocalization has remained controversial.[8,13−15] Although the original synthesis of the carbene was rationalized by assuming that delocalization of the nitrogen lone pairs into the empty p orbitals would stabilize the electron-deficient carbene center, the majority of early computational work concluded that this type of delocalization was negligible or, at best, only a minor stabilizing factor.[13] However, failure of these early calculations to identify significant π bonding between the C=C of the unsaturated ring carbons caused these publications to come under heavy scrutiny.[16]

The unusual stability of the silylenes and germylenes has been rationalized using several theories, including aromatic stabilization similar to that for the carbene analogues.[8] The structures of the germylene and silylene were studied by single-crystal X-ray diffraction (Si and Ge) and gas-phase electron diffraction (Si). The experimental structures show planar ring geometries, as would be expected for aromatic heterocycles. Aromatic germylene and silylene species are planar. The corresponding nonaromatic carbene,[7] silylene,[7] and germylene[9] show puckered ring geometries. The diffraction pattern of the unsaturated germylene revealed a planar ring structure, suggesting that there may be some aromatic ring delocalization.[11] Interpolation of the carbene and germylene structures suggests that the unsaturated silylene likely also has a planar ring geometry. Surprisingly, saturation of the carbon−carbon bond in the ring distorts the structure minimally, producing only a slight "twist" across the N−C−C−N bridge.[11]

Photoelectron spectroscopy (PES) and inner shell electron excitation spectroscopy (ISEELS) are electron spectroscopy techniques which are complementary probes of molecular electronic structure. PES probes the occupied electronic structure by measuring the ionization energies of valence electrons. Core excitation (by ISEELS ox X-ray absorption) probes the unoccupied electronic structure by exciting electrons from inner shell levels to the virtual levels of the ground state. Recently, photoelectron spectroscopy has been used to investigate the electronic structure of cyclic diaminocarbenes, -silylenes, and -germylenes to determine how their electronic structure is related to their unique stability.[17,18] Despite extensive computational and spectroscopic analysis, the contribution of aromatic stabilization in the carbenes, silylenes, and germylenes is still heavily debated. This core excitation study of cyclic diaminocarbenes, diaminosilylenes, and diaminogermylenes extends a previous detailed study which treated only the silylenes.[12] The present work extends our earlier study to other group members which assists spectral interpretation and the development of systematic links with molecular bonding. The corresponding tin(II) and lead(II) species continue to elude synthesis.

Core excitation spectroscopy, using either X-ray absorption or ISEELS, is an ideal method of analyzing the electronic structure of heterocyclic compounds, because each site can be probed individually. Core electron spectra are a sum of the individual core spectra of each atomic site. This, along with the greater ease of high-level calculations, makes compounds with a high degree of symmetry ideal targets for core electron excitation spectroscopy. In this regard, the *tert*-butyl-substituted cyclic diamino compounds **1C**, **1Si**, **1Ge**, **2C**, **2Si**, and **2Ge** are ideal (see Chart 1 for structures and nomenclature). These species can all be stored indefinitely, as long as air and moisture are excluded, and they are volatile enough to be analyzed in the gas phase. The spectra of **4C**, the hydrogenated tetravalent analogues of the saturated carbene, diazabutadiene (**5**), and its fully saturated analogue (**6**) were also recorded to assist with spectral interpretation. The spectra of the hydrogenated tetravalent silicon species **3Si** and **4Si** have been presented earlier.[12] The structures of these compounds are summarized in Chart 1. The ISEELS spectra of the carbenes, silylenes, and germylenes have been interpreted with the aid of ab initio calculations.

II. Experimental Section

A. Samples. The compounds of this study were obtained as previously described in the literature. The carbenes were obtained by reductive desulfurization of the corresponding thioureas with potassium in boiling THF.[7] The silylenes and germylenes were obtained by reductive dehalogenation of the corresponding dichlorosiloles[8] and dichlorogermoles.[9] The compounds were purified by vacuum sublimation. Due to their high sensitivity to air and moisture, all compounds were

(10) Denk, M. K.; Lennon, R.; Hayashi, R.; West, R.; Belyakov, A. V.; Verne, H. P.; Haaland, A.; Wagner, M.; Metzler, N. *J. Am. Chem. Soc.* **1994**, *116*, 2691. Denk, M.; Green, J. C.; Metzler, N.; Wagner, M. *J. Chem. Soc., Dalton Trans.* **1994**, *116*, 2405.
(11) Herrmann, W. A.; Denk, M. K.; Behm, J.; Scherer, W.; Klingan, F. R.; Bock, H.; Solouki, B.; Wagner, M. *Angew. Chem., Int. Ed. Engl.* **1992**, *31*, 1485. Veprek, S.; Prokop, J.; Glatz, F.; Merica, R.; Klingan, F.-R.; Herrmann, W. A. *Chem. Mater.* **1996**, *8*, 825.
(12) Urquhart, S. G.; Hitchcock, A. P.; Lehmann, J. F.; Denk, M. *Organometallics* **1998**, *17*, 2352.
(13) Arduengo, A. J., III; Rasika Dias, H. V.; Dixon, D. A.; Harlow, R. L.; Klooster, W. T.; Koetzle, T. F. *J. Am. Chem. Soc.* **1994**, *116*, 6812.
(14) Heinemann, C.; Müller, T.; Apeloig, Y.; Schwarz, H. *J. Am. Chem. Soc.* **1996**, *118*, 2023.
(15) Heinemann, C.; Herrmann, W. A.; Thiel, W. *J. Organomet. Chem.* **1994**, *475*, 73.
(16) Boehme, C.; Frenking, G. *J. Am. Chem. Soc.* **1996**, *118*, 2039.
(17) Denk, M. K.; Green, J. C.; Metzler, N.; Wagner, M. *J. Chem. Soc., Dalton Trans.* **1994**, 2405.
(18) Arduengo, A. J., III; Bock, H.; Chen, H.; Denk, M. K.; Dixon, D. A.; Green, J. C.; Hermann, W. A.; Jones, N. L.; Wagner, M.; West, R. *J. Am. Chem. Soc.* **1994**, *116*, 6641.

Chart 1. Divalent (1, 2) and Tetravalent (3, 4) Group IV Compounds and the Ligand Species (5, 6) Investigated in This Work[a]

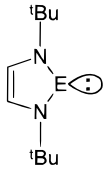

1C: E=C

1Si: E=Si

1Ge: E=Ge

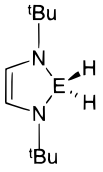

3C: E=C

3Si: E=Si

3Ge: E=Ge

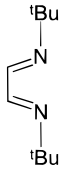

5

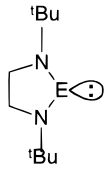

2C: E=C

2Si: E=Si

2Ge: E=Ge

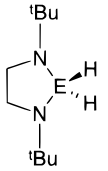

4C: E=C

4Si: E=Si

4Ge: E=Ge

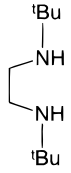

6

[a]The calculations were carried out on the corresponding species for which the ^{t}Bu groups are replaced by methyl groups. Throughout the text, these species are referred to as #c, #si, and #ge, where # = 1−4 as for the species studied experimentally.

handled and stored under an inert atmosphere (Ar or N_2) or vacuum and introduced directly into the collision chamber of the spectrometer via a short line from the valved storage vessel.

B. Inner Shell Electron Energy Loss Spectrometry. The ISEELS spectrometer[19,20] uses a beam of quasi monoenergetic electrons with impact energies in excess of 2500 eV to excite core excitation transitions in molecules in the gas phase. At the small scattering angles employed (2 ± 1°), the resulting spectra are dominated by electric dipole transitions; thus, they are very similar to the corresponding near-edge X-ray absorption spectra (NEXAFS). The method can be applied to any liquid or solid for which a vapor pressure greater than $\sim 1.0 \times 10^{-6}$ Torr can be obtained. The ISEELS spectrometer is routinely tuned using a standard calibrant gas (CO, CO_2, N_2) and operates with a typical full-width at half-maximum (fwhm) energy resolution of 0.7 eV. When it is calibrated using a gas mixture, as in this work, the energy loss scale is accurate to 50 meV. The electron beam is typically operated at 20−30 μA, with lower currents (2−4 μA) being used to record somewhat higher resolution spectra (∼0.5 eV fwhm) in the highly structured regions of the spectra.

Spectra are recorded as the sum of individual scans acquired by linearly sweeping over the energy loss region of interest. Approximately 6−30 h of scanning time was required to achieve acceptable statistics at each of the core edges investigated. The raw data were processed to produce the displayed spectra by removing the background signal, applying a kinematic correction, and establishing an absolute intensity scale by setting the core ionization oscillator strength in the continuum region to the atomic value using a standard documented procedure.[21] This procedure establishes an "oscillator strength per atom" scale, which is a weighted sum of all chemically distinct components. The absolute intensity scale was very helpful in this project, as it enabled dissection of overlapping spectral features through spectral stripping techniques.

C. Ab Initio Calculations. For the purposes of spectral assignment, ab initio calculations of the core excitation transitions were carried out using Kosugi's GSCF3 package.[22,23] Significant alterations in the electronic structure due to relaxation in core excited states make these high-level calculations necessary in order to reliably assign inner shell spectra.[24,25] These calculations are based on the improved virtual orbital approximation (IVO), which explicitly takes into account the core hole in the Hartree−Fock approximation. They are highly optimized for calculation of core excited states.[26] A separate calculation is performed for each core excited atom. The difference in the total energy between the core ionized and ground-state energies gives the core ionization potential (IP) with a typical accuracy of ∼1 eV. The absolute accuracy of the predicted ionization potential is dependent on the size of the basis set. However, the core state term values (TV = IP − E) are less dependent on the size of the basis set. Thus, in some cases, to facilitate comparison the calculated spectra were aligned to the experimental results using the lowest resolved transition in the experimental spectrum.

Optimized (minimum total energy) molecular geometries for the carbene, silylene, and saturated germylene species were determined using 6-31G* basis sets, calculated by Gaussian 94,[27] Spartan,[28] or GAMESS.[29] The optimized geometry calculated for **1Ge**, the unsaturated germylene, was in good agreement with that determined by single-crystal X-ray diffraction.[11] Methyl groups were used in place of the *tert*-butyl substituents in order to allow convergence in a reasonable calculation time. The *tert*-butyl substituents are not believed to be required for electronic stabilization of these compounds but, rather, act to prevent dimerization in the condensed phase. Replacement of the *tert*-butyl groups with smaller methyl substituents was therefore not expected to significantly alter conclusions drawn about the electronic structure of the heterocycle in the gas phase. This approximation has been used before with excellent results.[12] Lower case letters, using the same labeling scheme as the experimental spectra of the compounds, are used to identify the spectra calculated for the methyl-substituted species (see Chart 1). The geometry and basis sets used for the carbene, silylene, and germylene calculations are summarized in Table 1.

(19) Hitchcock, A. P. *Phys. Scr.* **1990**, *T31*, 159.
(20) Urquhart, S. G. Ph.D. Thesis, McMaster University, 1997.
(21) Hitchcock, A. P.; Mancini, D. C. *J. Electron Spectrosc.* **1994**, *67*, 1.
(22) Kosugi, N. *Theor. Chim. Acta* **1987**, *72*, 149.
(23) Kosugi, N.; Kuroda, H. *Chem. Phys. Lett*, **1980**, *74*, 490.
(24) Kosugi, N.; Shigemasa, E.; Yagishita, A. *Chem Phys. Lett.* **1992**, *190*, 481.
(25) Kosugi, N.; Adachi, J.; Shigemasa, E.; Yagishita, A. *J. Chem. Phys.* **1992**, *97*, 8842.
(26) Hunt, W. J.; Goddard, W. A., III. *Chem. Phys. Lett.* **1969**, *3*, 41
(27) Frisch, M. J.; Trucks, G. W.; Schlegel, H. B.; Gill, P. M. W.; Johnson, B. G.; Robb, M. A.; Cheeseman, J. R.; Keith, T.; Petersson, G. A.; Montgomery, J. A.; Raghavachari, K.; Al-Laham, M. A.; Zakrzewski, V. G.; Ortiz, J. V.; Foresman, J. B.;. Peng, C. Y.; Ayala, P. Y.; Chen, W.; Wong, M. W.; Andres, J. L.; Replogle, E. S.; Gomperts, R.; Martin, R. L.; Fox, D. J.; Binkley, J. S.;. Defrees, D. J.; Baker, J.; Stewart, J. P.; Head-Gordon, M.; Gonzalez, C.; Pople, J. A. Gaussian 94, Revision B.3; Gaussian, Inc., Pittsburgh, PA, 1995.
(28) Spartan 4.0; Wave function Inc., 18401 Von Karman Ave., #370, Irvine, CA 92715.
(29) Schmidt, M. W.; Baldridge, K. K.; Boatz, J. A.; Elbert, S. T.; Gordon, M. S.; Jensen, J. J.; Koseki, S.; Matsunaga, N.; Nguyen, K. A.; Su, S.; Windus, T. L.; Dupuis, M.; Montgomery, J. A. *J. Comput. Chem.* **1993**, *14*, 1347.

Table 1. Geometries and Basis Sets[a] Used for GSCF3 Calculations

	unsaturated			saturated		
distance/angle	**1c**[b]	**1si**[c]	**1ge**[c]	**2c**[b]	**2si**[c]	**2ge**[c]
			Bond Lengths (Å)			
E−N	1.352	1.742	1.839	1.341	1.720	1.818
N−C	1.385	1.390	1.383	1.455	1.456	1.454
C−C	1.333	1.332	1.335	1.532	1.536	1.531
C−H	1.069	1.071	1.072	1.085	1.089	1.090
N−Me	1.443	1.497[d]	1.467	1.437	1.489[c]	1.467
			Bond Angles			
N−E−N	102.5	86.3	83.6	105.6	89.2	86.4
E−N−C	112.5	114.6	114.4	114.9	116.3	115.0
E−N−Me	123.3	127.0	128.2	123.6	124.4	128.2
N−C−C	106.3	112.2	113.8	101.6	105.8	106.3
N−C−H	122.9	121.2	120.7	111.5	111.2	111.1
			Ring Torsion Angle			
E−N−CH_x∼CH_x	0.0	0.0	0.0	0.0	22.3	0.0[e]

[a] The following basis functions (Huzinaga et al.)[34] were used: 51 for H, 421/311 for C and N, 4321/421 for Si, and 4322/422/21 for Ge. On the atom on to which the core hole is placed, a more complex basis set expansion is used: 321111/21111/* for C and N, 3112121/311111/* for Si, and 211212121/312121/211/* for Ge. [b] From 6-31G* optimization of the methyl carbene structure. [c] From 6-31G* optimization of the structure with a H substituent on each N, followed by manually converting the H to a methyl group using reasonable N−C bond lengths. [d] These distances are the ones used in our previous study.[12] While clearly inconsistent with the optimized N−Me distances for the carbene and silylene species, we have found that the results are not affected by changes of 0.05 Å and thus prefer to use the same values as reported earlier. [e] In the solid state saturated germylene has a torsion angle of ∼5°.[11] However, the crystal structure indicates disorder, implying a low barrier to inversion. The 6-31G calculation reported a planar ring, but another approach gave a small torsion angle.

III. Results and Discussion

Molecules with conjugated π-bonding, aromatic systems, or even just isolated C=C or C=N double bonds, typically exhibit low-energy core excitation transitions due to the presence of one or more low-lying π^* molecular orbitals. If the stability of the molecule is increased by π delocalization, the $\pi-\pi^*$ separation increases, and thus the core → π^* transition increases in energy. Any delocalization in the divalent species, whether fully aromatic, or simply stabilization of the N−C−N allyl type (N → C π-back-donation) is expected to be manifested as a shift of the core → π^* transition to higher energy. Thus, the relative energy of low-lying core → π^* excitations provides information about the relative position of π^* levels and also the type and extent of multicenter interactions in the π manifold. The relative energy of the core → LUMO transition will also depend on the location of the core hole. In general, the energy (relative to the ionization threshold) is lower for core hole sites at which there is greater electron density in the upper orbital. Both the relative intensities and relative positions (term values) of excitations from different sites to the same unoccupied orbital provide information about the spatial distribution of excited electron density in that orbital.

The above discussion summarizes our perspective on using core excitation spectra to "map" the unoccupied electronic structure of related series of molecules. Of course, the nature of the occupied energy levels is of greater general interest. Several assumptions must be valid in order to determine information about the occupied electronic structure from details of the unoccupied electronic structure as sampled by core excitation. First, the occupied and unoccupied orbital manifolds are assumed to be complementary. Second, core hole relaxation effects must be similar at all sites in all molecules. These are the starting points for our spectral interpretation outlined in the following sections, which are grouped according to core edge. This study generalizes the result of our previous silylene study[12] by showing that the N 1s edge is the core level most sensitive to the extent of delocalization.

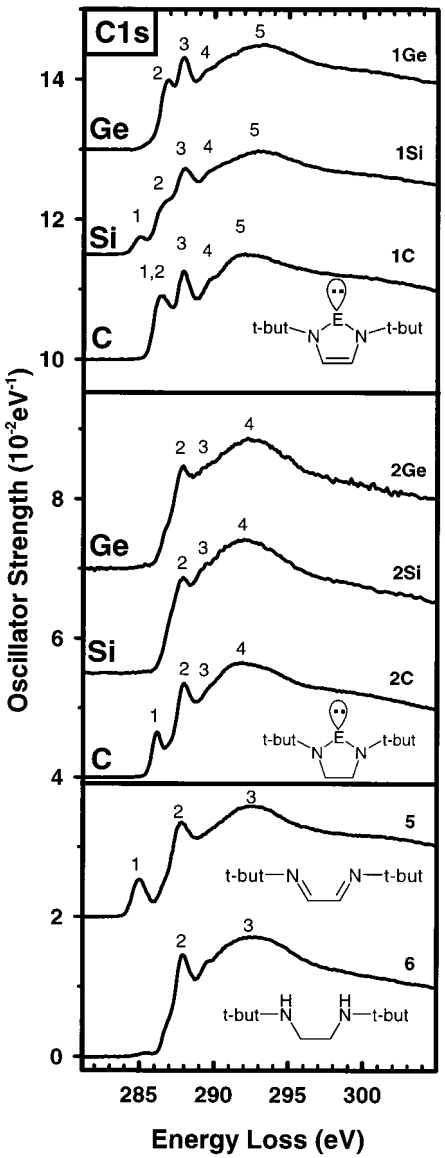

Figure 1. Carbon 1s oscillator strength spectra of the divalent species **1** and **2** compared to those of the ligand species **5** and **6**. These spectra are derived from inner shell energy loss spectra recorded under experimental conditions dominated by electric dipole transitions (2500 eV final electron energy, 2° scattering angle) and thus are expected to be very close to the corresponding near-edge X-ray absorption (NEXAFS) spectra.

A. C 1s Spectra. The C 1s oscillator strength spectra of the saturated and unsaturated diaminocarbenes **1C** and **2C**, diaminosilylenes **1Si** and **2Si**, diaminogermylenes **1Ge** and **2Ge**, and molecules approximating the "ene ligands" (**5**, **6**) are shown in Figure 1. The energies and proposed assignments of the observed features in the ligands **5** and **6** and in **4C**, the tetrava-

Table 2. Peak Energies and Proposed Assignments for Features in the C 1s and N 1s Spectra of 4C, 5, and 6

C 1s

	species			assignt (final level)	
peak no.	**4C**	**5**	**6**	CH_x	^{t}Bu
1	-	285.0		π^*_{CN} a_2	
1′ sh	-	286.4	286.6		3s Rydberg
2	288.0[a]	288.0(1)[a]	288.0[a]		σ^*_{CH}
2′ wk			289.6(2)		3p Rydberg
3 br	291.6(5)	293	293		σ^*_{CC}
4 br		302		σ^*_{CN}	

N 1s

	species			
peak no.	**4C**	**5**	**6**	assignt (final level)
1		398.19(8)[b]		$1\pi^*_{CN}$
2		401.4		$2\pi^*_{CN}$
2′	401.6		401.1	3s Rydberg
3 br	404.2[b]	405.5	405.1[b]	σ^*_{CN}
3′ br	409(1)			σ^*_{CN}
4 br		412		$\sigma^*_{C=N}$

[a] Calibration: **4C**, −2.7(1) eV relative to CO_2 π^*; **5**, −2.72(8) eV relative to CO π^*; **6**, −2.7(1) eV relative to CO_2 π^*. [b] Calibration: **4C**, +3.1(1) eV relative to N_2 π^*; **5**, −2.95(5) eV relative to N_2 π^*; **6**, +4.0 (1) eV relative to N_2 π^*.

Table 3. Peak Energies (eV) and Proposed Assignments for Features in the C 1s Spectra of the Divalent Unsaturated Species 1C, 1Si, and 1Ge

peak	species			assignt (final level)		
no.	**1C**	**1Si**	**1Ge**	>C:	C=C	^{t}Bu
1	285.9				π^* a_2	
1	286.44(8)[b]	285.01[a]		π^* b_2	π^* b_2	
2		286.6	286.86(8)		π^* a_2	
3	287.89(6)[a]	288.0	286.90(8)[a]			σ^*(C−H)
4 wk	289.9(1)	289.6	289.6(2)			
5 br	292.1(2)	293	291.1(1)			σ^*(C−C)
6 br	302	302	302		σ^*(C=C)	

[a] Calibration: **1C**, −2.85(5) eV relative to CO_2 π^*; **1Si**, −2.32 eV relative to CO π^*; **1Ge**, −3.84(5) eV relative to CO_2 π^*. [b] From spectral stripping: see Figure 2 and text.

Table 4. Peak Energies (eV) and Proposed Assignments for Features in the C 1s Spectra of the Divalent Saturated Species 2C, 2Si, and 2Ge

peak	species			assignt (final level)		
no.	**2C**	**2Si**	**2Ge**	>C:	C−C (ring)	^{t}Bu
1	286.1		-	π^* b_2		
2	287.90(8)[a]	287.93(8)[a]	287.88(8)[a]		σ^*_{CH}	σ^*_{CH}
3 wk	289.8(3)	289.6	289.5(3)			
4	292	292	292		σ^*_{CC}	σ^*_{CC}

[a] Calibration: **2C**, −2.84(5) eV relative to CO_2 π^*; **2Si**, −2.81(5) eV relative to CO_2 π^*; **2Ge**, −2.86(5) eV relative to CO_2 π^*.

lent saturated carbene analogue, are summarized in Table 2. Energies and proposed assignments for the C 1s spectra of the unsaturated species **1C, 1Si,** and **1Ge** are listed in Table 3, while those for the saturated species **2C**, **2Si**, and **2Ge** are listed in Table 4.

To use core spectra to explore the electronic structure of the divalent compounds **1** and **2,** it helps to consider the core excitation spectra of the "ligand" to the divalent site (E^{II}) prior to the addition of the divalent atom. The diazabutadiene was studied as a ligand model for the unsaturated species **1** and the diazabutane as a model for the saturated species **2**. The 1,4-diaza-2-butene ^{t}BuNHCH=CHNH^{t}Bu would have been the first choice to model the ligand properties in **1**, but the NHCH=C fragment would make this compound unstable to tautomerization to ^{t}BuN=CHCH$_2$NH^{t}Bu. Attempts to generate the 1,4-diaza-2-butene in situ from silylated precursors and alcohols or water were unsuccessful.[35] The 1,4-diaza-1,3-butadiene ^{t}BuNH=CHCH=N^{t}Bu was chosen instead. The C 1s spectrum of diazabutadiene **5** (lowest panel, Figure 1) has a low-lying transition at 285.0 eV, which is assigned to C 1s → $1\pi^*_{CN}$ transitions. (In our notation convention we use a subscript to the upper orbital designation to indicate the location of the main electron density in that orbital. For example, in the **s**pecies **1**, this allows us to distinguish the π^*_{CC} a_2 level, with mainly C=C character, from the π^*_{CN} b_2 level, which is mostly localized at the N−E^{II}-N end of the ring. Where there is no confusion, the additional subscript labeling is dropped.) The second feature, at ∼288 eV, is present in all C 1s spectra reported in this work, and thus it is easily identified as being characteristic of the *tert*-butyl substituents, common to all species. The *tert*-butyl groups are not part of the π-system and, accordingly, do not display any characteristic shifts. The spectrum of the completely saturated ligand **6** is very similar to that of **5**, except that there is no low-lying 285 eV feature, as expected from the absence of a π^* level in **6**.

The C 1s spectra of the unsaturated (**1**) and saturated (**2**) divalent species exhibit some significant differences from the spectra of the ligand models **5** and **6**. From the earlier study of silylenes,[12] a low-lying feature associated with excitation to the π^* b_2 level was expected in each of the unsaturated species, assuming ring delocalization. In the unsaturated silylene **1Si** this feature occurs at 284 eV. It is shifted to higher energy and has lower intensity relative to the strong π^* feature in the C 1s spectrum of the ligand **5**. This reflects a much smaller degree of delocalization in **1Si** than in **5**. The presence of this transition clearly indicates that the unsaturated silylene contains some C=N double-bond character, consistent with N−Si−N π-allyl and aromatic delocalization, as previously discussed.[12]

In contrast to **1Si,** a low-lying transition was not observed in the carbon 1s spectrum of either **1C** or **1Ge.** At first consideration, this was very surprising. However, the rationalization for this provides useful insight into the effect of changing from C: to Si: to Ge: in these species. On the basis of orbital overlap (both in terms of size and energy relative to the ligand N 2p orbitals), the carbenes **1C** and **2C** are expected to be significantly more delocalized than the silylenes or germylenes. This would tend to increase the π−π^* separation, which shifts the C 1s(C=C) → π^*_{CN} b_2 transition in the carbene **1C** to higher energy, where it overlaps other levels, in particular the C 1s(>C:) → $\pi^*_{C=C}$ a_2 transition at 285 eV. In the unsaturated germylene **1Ge** the C 1s(C=C) → π^*_{CN} b_2 transition, if present, is very weak (see discussion below). This transition is believed to be weak or absent because there is very little C=N double-bond character (i.e. little aromatic delocalization) in this species.

The lowest energy transition in **1C** occurs at 286.4 eV, at about the same energy but significantly more intense than the corresponding lowest energy transition in **2C**. In the saturated species **2C**, this feature is clearly

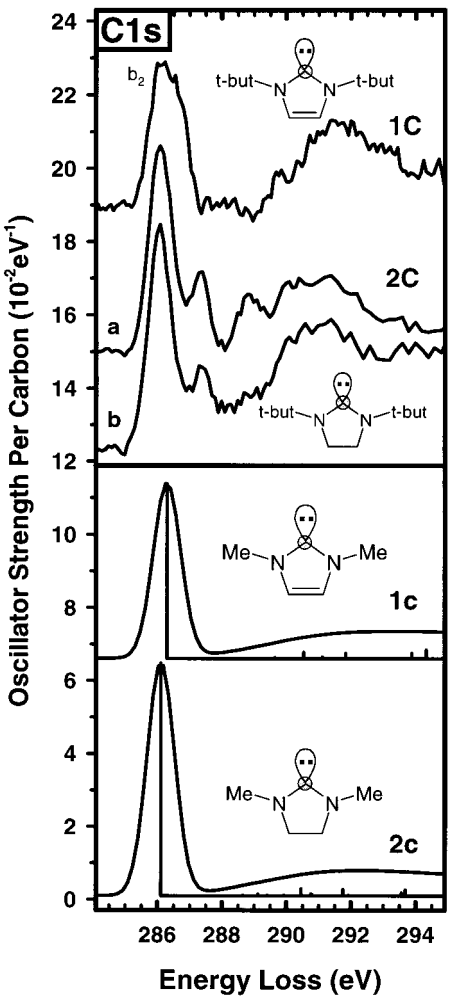

Figure 2. (top) C 1s spectra of the divalent carbon site of **1C** and **2C** generated by spectral stripping. Curve a is the difference of the C 1s spectra of **2C** and **6**, accounting for the presence of 12 carbons in **6** and 13 carbon atoms in **2c**. Curve b for **2C** and that for **1C** were derived by using the C 1s spectra of the saturated (**4Si**) and unsaturated (**3Si**) tetravalent silicon analogues to approximate the nondivalent carbon sites, and subtracting these spectra from the spectrum of each carbene generates the spectrum of the "naked carbene". (bottom) Calculated spectra of the divalent carbon site in **1c** and **2c** (with methyl groups instead of ^{t}Bu groups). The calculated spectra have been shifted to align them with the experimental data at the lowest energy transition (shifts: **1c**, −2.0 eV; **2c**, −2.6 eV).

the C 1s(>C:) → π^* b_2 transition at the divalent site. It is well-resolved, since there is no overlapping C═C double-bond contribution. The greater intensity of feature 1 in **1C** relative to feature 1 in **2C** is the clue indicating that the expected C 1s(C═C) → π^* b_2 and C 1s(>C:) → π^* b_2 transitions overlap. The intensity of the C 1s(>C:) → π^* b_2 component in **1C** and **2C** can be estimated by subtracting the spectra of the tetravalent silylenes **3B** and **4B**[12] from **1C** and **2C**, respectively. Alternatively, for the saturated species the C 1s(>C:) component can be estimated by subtracting the spectrum of the saturated ligand (**6**) from that of **2C**. These approaches are explored in Figure 2, which also compares these experimental estimates of the C 1s spectrum of the divalent C: site to the spectra predicted by the calculations. In both **1C** and **2C** the isolated spectrum of the divalent site exhibits a strong transition around

Table 5. Peak Energies and Proposed Assignments for the N 1s Spectra of the Divalent Unsaturated Species 1C, 1Si, and 1Ge[a]

peak no.	1C	1Si	1Ge	assignt
1	401.8(1)	400.0	399.52(8)	π^* b_2
2		402.0	401.87(8)	σ^*_{EN} b_1
3	404.4(2)		404.5(2)	
4	406.2(2)	406	406.3(2)	

[a] Calibration: **1C**, −2.84(5) eV relative to CO_2 π^*; **1Si**, −2.81(5) eV relative to CO_2 π^*; **1Ge**, −2.86(5) eV relative to CO_2 π^*.

Table 6. Peak Energies and Proposed Assignments for the N 1s Spectra of the Divalent Saturated Species 2C, 2Si, and 2Ge[a]

peak no.	2C	2Si	2Ge	assignt
1	400.9(1)	399.6	398.97(8)	π^* b_2
2		401.8	401.4(1)	σ^*_{EN} b_1
3	402.2(2)		402.1(1)	
4	405.1(3)	404	406.2(3)	

[a] Calibration: **2C**, −2.84(5) eV relative to CO_2 π^*; **2Si**, −2.81(5) eV relative to CO_2 π^*; **2Ge**, −2.86(5) eV relative to CO_2 π^*.

286 eV, which is assigned to the C 1s(>C:) → π^* b_2 transition. The strong oscillator strength indicates a large C $2p_z$ character at the C: site, consistent with the theoretical predictions.

The most intense C 1s signals, labeled 2, 3, and 4 in the **2** species and 3, 4, and 5 in the **1** species, are attributed to C 1s → σ^*_{C-H} and C 1s → σ^*_{C-C} transitions at the *tert*-butyl substituents. Due to their fully saturated character and electronic isolation from the heterocyclic ring, the *tert*-butyl component exhibits essentially no energy loss shifts or intensity changes and can therefore be modeled well by 2-methylpropane.[30]

It is interesting to compare the C 1s spectra of the divalent C: site in **1C** to the Si 1s spectra of the divalent Si: site in **1Si** and to the Ge 1s spectra of the divalent Ge: site in **1Ge**. This comparison is facilitated by subtraction of the signals from all other carbon atoms in **1C** as well as by comparison to the results of the GSCF3 ab initio calculations. The isolated spectra of the divalent sites in **1C** and **1Si** are presented in Figure 3, along with plots of the relevant molecular orbitals (MOs) in **1c, 1si**, and **1ge**. The key calculational results for **1c, 1si,** and **1ge** are summarized in Table 7, while those for **2c, 2si,** and **2ge** are summarized in Table 8. Only computational data are available for Ge 1s excitation of **1ge**, since Ge 1s measurements have not been made on the **1Ge** species.

As indicated in Figure 3, the computational results are in good agreement with experimental results for the spectra of the divalent sites. Both experiment and theory indicate there is considerable similarity of the energies and spatial distributions of the LUMO in all three species and also between the LUMO{+1} in the silylene and germylene. However, the unoccupied electronic structure of the carbene is qualitatively different. In particular, the calculations for **1c** indicate the LUMO{+1} orbital has no contribution at the divalent site. The orbital in the C 1s(>C:) core excited **1c** species, which is closest in shape to that of the b_1 LUMO{+1} in **1Si** and **1Ge**, is in fact 6 eV at higher energy (and is that plotted in Figure 3). It may correspond to the signal detected experimentally around 292 eV. A consideration

(30) Hitchcock, A. P.; Ishii, I. *J. Electron Spectrosc.* **1987**, *42*, 11.

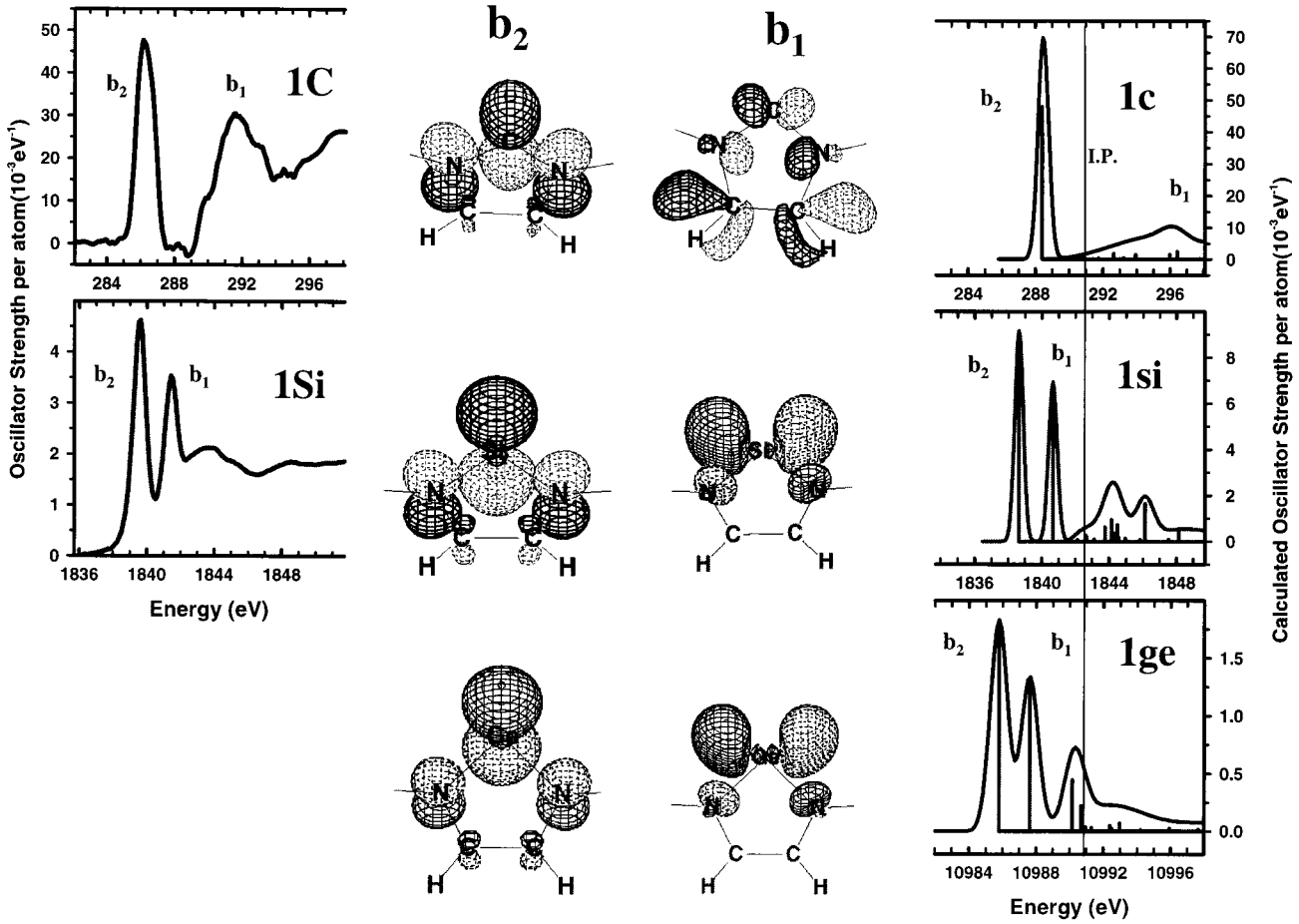

Figure 3. Comparison of experimentally derived spectra of the 1s excitation at the divalent site in **1C** and **1Si** with the spectra predicted for this site from ab initio improved virtual orbital (IVO) calculations for **1c**, **1si**, and **1ge**. The MO plots are those of the LUMO and LUMO{+1} for the 1s core excited divalent site of **1si** and **1ge**. The b_1 orbital plotted for **1c** is located much higher in the manifold of unoccupied levels. The LUMO{+1} orbital of **1c** is ring σ^*(C−N) in character and has no contribution from the in-plane 2p orbital at the C: divalent site. The vertical bar indicates the position of the calculated core IP. Note that the spectrum for 1C is a smoothed version of that presented in Figure 2. Also, a different scale factor was used, to allow easier comparison to the Si 1s spectrum of **1si**.

Table 7. Calculated Results for Excitation of Unsaturated Carbene, Silylene, and Germylene

site/peak no.	sym	IP	ϵ (eV)	f
A. C 1s Excitation of Unsaturated Carbene **1c**[a]				
divalent C 1s	b_2	290.861	−2.33	0.0557
	b_1		+5.40	0.0121
ring C 1s	a_2	291.233	−2.54	0.0237
	b_2		−1.31	0.0031
N 1s	b_2	405.487	−1.64	0.0114
B. Si 1s, C 1s, and N 1s Excitation of Unsaturated Silylene **1si**[a]				
Si 1s	b_2	1842.43	−3.81	0.0058
	b_1		−1.81	0.0044
ring C 1s	b_2	290.623	−2.41	0.0071
	a_2		−1.68	0.0157
N 1s	b_2	403.843	−3.09	0.0073
	b_1		−1.33	0.0006
C. Ge 1s, C 1s, and N 1s Excitation of Unsaturated Germylene **1ge**[a]				
Ge 1s	b_2	10963.3	−4.19	0.00094
	b_1		−2.29	0.00086
C 1s	b_2	290.496	−2.76	0.0044
	a_2		−1.36	0.0203
	b_1		−0.87	0.0037
N 1s	b_2	403.815	−3.52	0.0069
	b_1		−1.33	0.0010

[a] Only the most spectroscopically significant orbitals are listed.

Table 8. Calculated Results for C 1s and N 1s Excitation of Saturated Carbene, Silylene, and Germylene

site/peak no.	sym	IP	ϵ (eV)	f
A. C 1s and N 1s Excitation of Saturated Carbene **2c**[a]				
divalent C 1s	b_2	291.437	−2.67	0.0708
	b_1		+3.07	0.0072
ring C 1s	b_2	291.897	−1.88	0.0040
	C−H		−1.28	0.0070
N 1s	b_2	404.704	−1.08	0.0035
B. Si 1s, C 1s, and N 1s Excitation of Saturated Silyene **2si**[a]				
Si 1s	b_2	1842.88	−4.38	0.0078
	b_1		−1.69	0.0040
ring C 1s	b_2	291.509	−2.28	0.0004
	C−H		−1.48	0.0046
N 1s	b_2	403.525	−2.97	0.0041
	b_1		−0.98	0.0004
C. Ge 1s, C 1s, and N 1s Excitation of Saturated Germylene **2ge**[a]				
Ge 1s	b_2	10963.7	−4.80	0.00132
	b_1		−2.31	0.00074
C 1s	b_2	291.271	−2.62	0.0004
	b_1		−1.39	0.0048
	C−H		−0.61	0.0085
N 1s	b_2	403.066	−3.35	0.0038
	b_1		−1.06	0.0007

[a] Only the most spectroscopically significant orbitals are listed.

of atomic energies suggests the reason for this difference. For E = Si, Ge, the $(n + 1)$p levels (which occur in the ground state calculation at +6.6 eV in Si and +6.5 eV in Ge) significantly contribute to the LUMO{+1} and

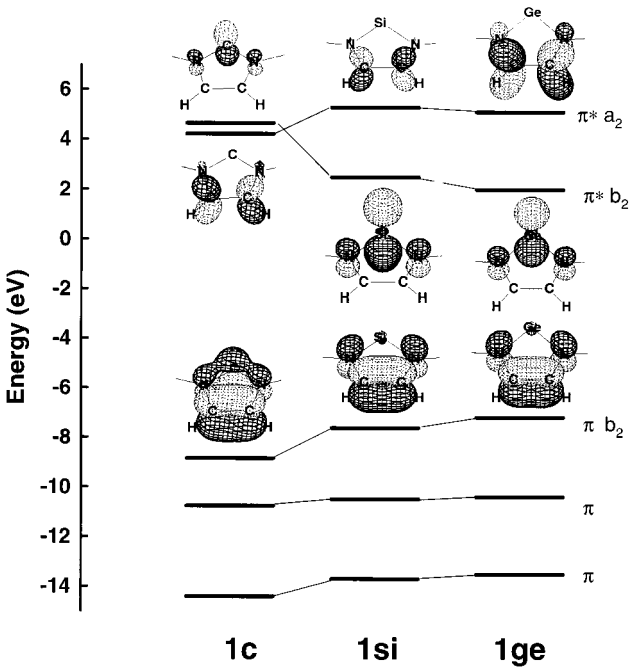

Figure 4. Molecular orbital diagram and orbital plots for the π manifold of the unsaturated species, as predicted by the ground-state calculations for **1c**, **1si**, and **1ge**.

thus make these orbitals delocalized. For E = C, the (n + 1)p orbital (which lies at +9.5 eV in the GSCF3 ground-state calculation with the same, large basis set) does not contribute significantly. In the core excited states the (n + 1)p orbitals contribute to the low-lying b_1 LUMO{+1}, whereas they contribute to a much higher energy MO in the carbene.

It is also instructive to compare the ground-state orbital energies for the π manifold (Figure 4)**.** There is a crossover in the ordering of the a_2 and b_2 orbitals, with the $\pi^*_{C=C}$ a_2 level lying below the b_2 level in the carbene. The calculations also clearly show that the b_2 level shifts to lower energy in the sequence C−Si−Ge (ϵ is −2.62, −3.85, and −4.19 eV, respectively), and thus the E: excitation to the b_2 level will shift to lower relative energy (i.e. larger term value) in this sequence. This is consistent with an enhanced π−π^* splitting associated with a larger aromatic character in the carbene relative to the silylene or germylene. The stronger interaction between the $2p_z$ orbital at C: and the $2p_z$ orbitals of the adjacent nitrogen atoms results in a greater spatial overlap and larger N $2p_z$ contribution in the series carbene > silylene > germylene for E 1s → LUMO excitation.

The situation for the saturated divalent species **2C, 2Si,** and **2Ge** is very similar to that for the unsaturated species. The LUMO orbital shapes for core excitation at the divalent site in the saturated species (not shown) are remarkably similar to those in the unsaturated species, except for elimination of the small contributions from the $2p_z$ orbitals at the C−C ring atoms. The calculated and experimental Si 1s spectra of **2Si** as well as the calculated spectrum of **2ge** exhibit two lines, whereas the calculated and experimental spectra of **2C** exhibit only a single sharp low-lying line. Again we attribute the lack of the second low-lying line in the C 1s(>C:) spectrum of **2C** to the difference in the energies of the atomic (n + 1)p orbitals.

The oscillator strength (f) of the low-lying (>C:) → π^* b_2 transition is smaller in **1C** (f = 0.051) than in **2C** (f = 0.071), indicating a greater delocalization of the out-of-plane 2p orbital at the C: site in **1C**. The well-resolved peaks isolated by spectral stripping (Figure 2) show that the C 1s(>C:) → π^*b_2 transition for **1C** is shifted 0.2 eV higher in energy than that of **2C** (286.0 eV). This upward shift indicates an increased stability in **1C** relative to **2C** due to aromatic and/or geometric stabilization. Compounds **1C** and **1Ge** have C_{2v} symmetry in the solid state,[7,9] while **2C** and **2Ge** have C_2 geometries.[9,11] Since the twists in the ring are minimal and likely to be fluxional in the gas phase, C_{2v} transition symmetries have been used for convenience when discussing compounds **1** and **2**.

Spectral subtraction was also used to isolate the C 1s spectral features associated with the ring carbons in **1C**, **1Si**, and **1Ge**. The *tert*-butyl contributions to the measured spectra were removed by subtracting the C 1s spectrum of 2-methylpropane.[30] The C 1s spectral component of the C=C double bond of the unsaturated species **1** was estimated by subtracting first the C 1s spectrum of 2-methylpropane (taking into account numbers of sites), and then the divalent contribution in the case of **1C**. The results of this analysis are presented in Figure 5. In addition, the calculated spectra of the C=C ring carbons are plotted. The isolated C=C component of the carbenes **1C** and **1c** exhibits only a single low-lying feature at 286.0 eV of high intensity, suggesting that the π^* a_2 electron density is localized in the C=C region. The unsaturated silylene **1Si** exhibits two low-lying transitions associated with excitation at the C=C atoms of the ring, consistent with aromaticity and a considerable amount of C=N ring π-bonding. The greater intensity of the higher energy feature (E = 286.4 eV, f = 0.043) is also consistent with electron density transfer from the electron-rich nitrogen centers to the C=C double-bond region through a π-bond. The C 1s-(C=C)→ π^*_{CN} b_2 transition is observed above the C 1s-(C=C) → π^* a_2 transition as a weak but distinct feature in the spectrally isolated C 1s spectrum of the unsaturated carbene **1C**. The fact that it comes higher rather than lower than the main C 1s(C=C) → π^* a_2 transition is consistent with the orbital ordering predicted by the calculations and a greater delocalization in the carbene, as is also evident in the spectroscopy and calculations for the C 1s(>C:) site. In completing our discussion of Figure 5, we note that the calculated and measured C 1s spectra of the germylene do not agree in terms of the relative strength of the lowest energy feature. However there is a weak low-energy shoulder in the C 1s(C=C) spectrum isolated for **1Ge**, which may be the experimental counterpart to the rather larger, lowest energy feature in the calculation of **1ge**.

Further information about the effect of the divalent carbon atom on the electronic structure of the carbene heterocycle is obtained by comparison of the spectrum of **2C** to the core spectra of the hydrogenated tetravalent carbon analogue **4C**. The C 1s and N 1s spectra of **2C** and **4C** are presented in Figure 6. The N 1s spectra are discussed in the following section. The divalent center in **2C** causes a new spectral feature at 286 eV, which is assigned to the 1s(>C:) → π^* b_2 transition; the band at next higher energy, assigned to C 1s(>C:) → σ^*_{C-H}, is

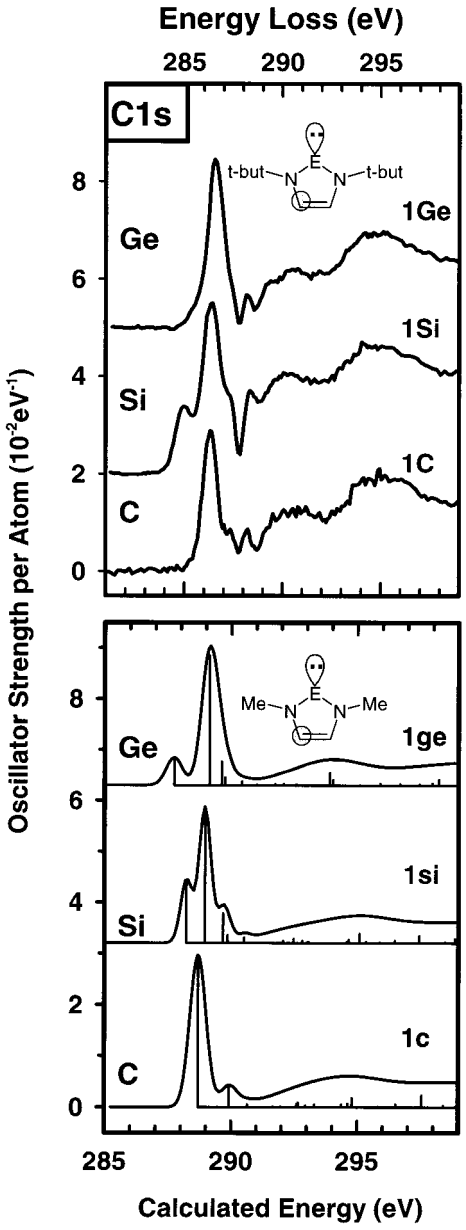

Figure 5. (top) C 1s contribution of the C=C sites in the unsaturated "enes" **1** derived from the experimental data by spectral stripping (see text for details). (bottom) C 1s spectrum of the C=C site predicted from the ab initio IVO calculations. The calculated spectra are presented on the calculated absolute energy scale, which is about 2.4 eV higher than the experimental values.

narrowed. As expected, C 1s(CH_2) → π^* b_2 transitions are absent in all saturated divalent species (**2C**, **2Si**, **2Ge**) (Figure 1). We also attempted to study the unsaturated tetravalent carbene analogue, since it is an ideal molecule with which to probe the effect of the divalent site in the unsaturated carbene. However, the tetravalent analogue polymerized too quickly for spectroscopic study.

B. N 1s Spectra. The N 1s spectra of the unsaturated species **1C**, **1Si**, and **1Ge** and saturated species **2C**, **2Si**, and **2Ge** and those of the ligands **5** and **6** are presented in Figure 7. The energies and proposed assignments for the nitrogen 1s spectral features are summarized in Tables 5 (unsaturated) and 6 (saturated). We consider the spectra of the two ligand species first. The N 1s

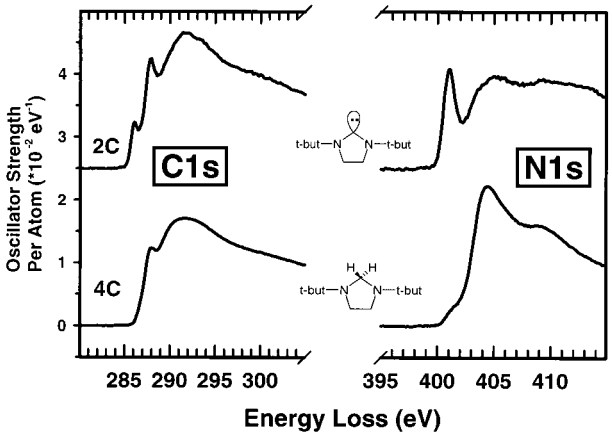

Figure 6. (left) C 1s and (right) N 1s spectra of the fully saturated hydrogenated (tetravalent) carbene analogue **4C** (bottom) contrasted with those of the carbene **2C** (top). Comparison of these two species allows unambiguous assignment of the lowest lying feature in **2C** to C 1s(>C:) → π^* b_2 excitation at the divalent carbon.

spectrum of the diazabutadiene **5** exhibits a strong low-energy N 1s → $1\pi^*_{CN}$ transition at 398.2 eV. This feature is the N 1s counterpart to that at 286 eV in the C 1s spectrum of **5**. A second, much less intense transition at 401.4 eV is assigned to the N 1s → $2\pi^*_{CN}$ transition. As in other compounds containing conjugated double bonds such as butadiene,[31] the transition to the lowest π^* level is the most intense spectral line and transitions to higher lying π^* levels are considerably weaker. This is a consequence of core hole relaxation.[32] As expected, the strong N 1s → π^*_{CN} transition is absent in the saturated ligand **6**. Instead, the lowest energy feature in **6** is a weak one at 401 eV, which is likely the N 1s excitation to the lowest 4s Rydberg state. The main peak in the N 1s continuum of **6** is rather close to the estimated ionization limit, whereas the maximum in the N 1s continuum of **5** is at much higher energy. These observations are readily explained by attributing these continuum maxima to shape resonances whose relative positions reflect the short N−C bonds in **5** and the longer N−C bonds in **6**.[33]

Comparison of the nitrogen 1s spectra of both unsaturated (**1**) and saturated (**2**) divalent species as a function of the nature of the divalent center (Figure 7) reveals some interesting similarities and differences. There is a striking resemblance of the silylene and germylene N 1s spectra, but the N 1s spectra of the carbenes **1C** and **2C** differ in that the lowest energy feature is shifted to significantly higher energy, and there is only one rather than two low-lying features. In all six species, the low-lying, relatively intense feature is attributed to N 1s → π^* b_2 transitions. The energy of this transition increases in the order germylene <

(31) Hitchcock, A. P.; Beaulieu, S.; Steel, T.; Stöhr, J.; Sette, F. *J. Chem. Phys.* **1984**, *80*, 3927 (84). Naves de Brito, A.; Svensson, S.; Correia, N.; Keane, M. P.; Agren, H. *J. Electron Spectrosc.* **1992**, *59*, 293.
(32) Oji, H.; Mitsumoto, R.; Ito, E.; Ishii, H.; Seki, S.; Yokoyama, T.; Ohta, T.; Kosugi, N. *J. Chem. Phys.* **1998**, *109*, 10409.
(33) Sette, F.; Stöhr, J.; Hitchcock, A. P. *J. Chem. Phys.* **1984**, *81*, 4906.
(34) Huzinaga, S.; Andzelm, J.; Klobokowski, M.; Radzio-Andzelm, E.; Sasaki, Y.; Tatewaki, H. *Gaussian Basis Sets for Molecular Calculations*; Elsevier: Amsterdam, 1984.
(35) Denk, M. Unpublished results.

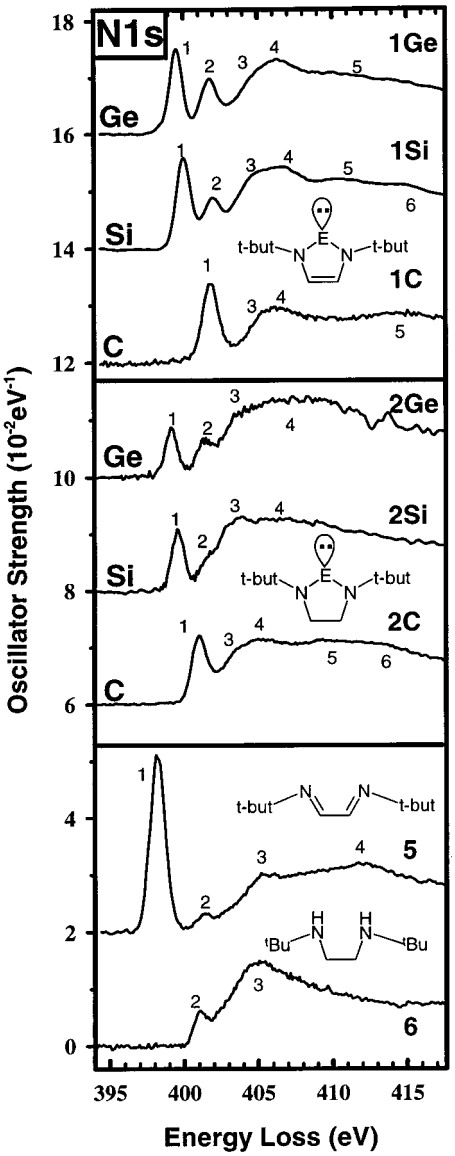

Figure 7. Nitrogen 1s oscillator strength spectra of the divalent species **1** and **2** compared to those of the ligand species **5** and **6**. See the caption to Figure 1 for details of the experimental conditions.

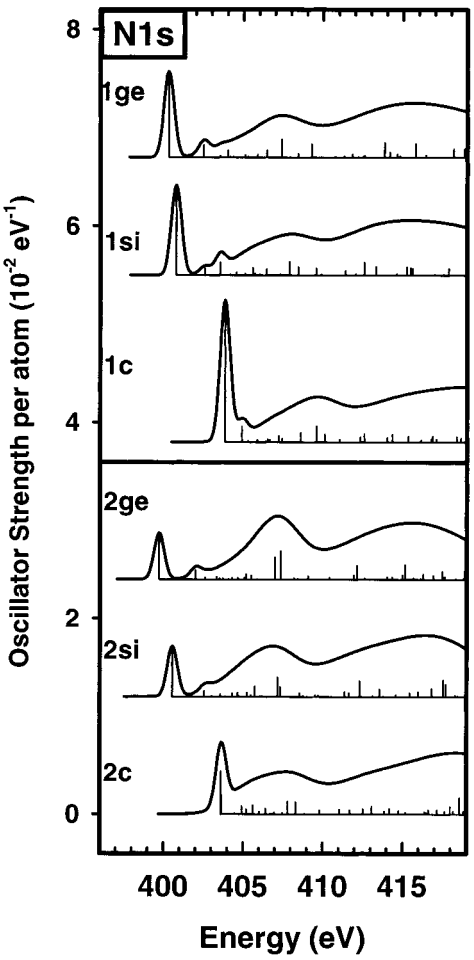

Figure 8. Ab initio calculated spectra of the N 1s edge of **1c**, **1si**, **1ge**, **2c**, **2si**, and **2ge.** The spectra are presented on the calculated absolute energy scales.

silylene < carbene (Tables 5 and 6). This may be related to the extent of delocalization in the π^* b_2 orbital, although it may also be the result of increasing electronegativity through the series. The second peak in the N 1s spectra of the silylenes **1Si** and **2Si** and germylenes **1Ge** and **2Ge** is attributed to N 1s $\rightarrow$ σ^*_{EN} b_1 transitions, which involve in-plane interactions of 2p orbitals (see MO plots in Figure 3). In the carbenes **1C** and **2C** the corresponding carbon atomic orbital is sufficiently high that there is no longer a low-lying σ^*_{EN} b_1 orbital and thus no corresponding N 1s transition.

The difference in the electronic structure of the saturated divalent species **2** relative to that of the unsaturated species **1** is very clear at the N 1s edge. The b_2 transition in **2Ge** becomes significantly less intense than in **1Ge**, suggesting a change in the nitrogen electronic structure, perhaps associated with less overlap of the E: $2p_z$ and the N $2p_z$ orbital. Alternatively it could be associated with a slight twist through the N−C−C−N bridge of the saturated species **2**. The drop in b_2 intensity from **1** to **2** is most pronounced for the germylenes, suggesting it is associated with reduced delocalization. The lowest energy N 1s $\rightarrow$ π^* b_2 transition in the saturated carbene **2C** is 0.9 eV lower than the corresponding b_2 transition in **1C**, whereas the energies of the N 1s $\rightarrow$ π^* b_2 transitions in the saturated and unsaturated silylene and germylene species differ by a smaller amount (0.4 eV) (see Tables 5 and 6). This suggests that delocalization in the π^* b_2 orbital all around the ring is of greatest importance in the unsaturated carbene **1C** and of less importance in the silylene **1Si** and germylene **1Ge**. At the same time, notwithstanding the shifts in intensity and energy noted above, for each species (C, Si, Ge), the N 1s spectra of the unsaturated (**1**) and saturated (**2**) compounds are relatively similar, suggesting that there is a similar level of E^{II}−N delocalization through the N−C^{II}−N, N−Si^{II}−N, and N−Ge^{II}−N region in each of the pairs **1C**/**2C**, **1Si**/**2Si**, and **1Ge**/**2Ge**. This could explain why the observed transition energy increases in the order germylene < silylene < carbene almost as much in the saturated species as in the unsaturated species.

It is also interesting to compare the N 1s spectrum of the saturated carbene **2C** with that of the tetravalent analogue **4C** (Figure 6). In the nitrogen 1s spectrum, the lowest lying feature, corresponding to N 1s $\rightarrow$ π^* b_2 transitions in **2C,** completely disappears in **4C**. Its absence clearly indicates that there is delocalization through the divalent site in **2C**. The experimentally

derived oscillator strengths of the N 1s → π^* b_2 transitions in **2C**, **2Si**, and **2Ge** are 0.015, 0.011, and 0.007, respectively. This suggests that the extent of $NE^{II}N$ (E^{II} = C, Si, Ge) delocalization is greatest for the carbene and lowest for the germylene. This is consistent with the trends expected from the match of the N 2p orbital size and energy with that of the outermost *n*p orbital of the E^{II} "ene" atom.

The calculated N 1s spectra of **1c**, **1si**, **1ge**, **2c**, **2si**, and **2ge** are presented in Figure 8. The calculated spectra are presented using the absolute calculated transition energies, which are systematically about 2 eV higher than those measured experimentally. Overall, the calculated spectra are in remarkably good agreement with the experimental spectra (Figure 7). They clearly show a systematic shift of the lowest lying π^* b_2 transition to higher energy in the germylene, silylene, carbene series and confirm that the carbene species has a simpler low-lying spectrum. The calculated π^* b_2 transitions are similar in intensity in the unsaturated silylene **1si** and germylene **1ge**, whereas the unsaturated carbene **1c** has a significantly larger oscillator strength. This is clear evidence for the contribution of additional aromatic delocalization in **1c**.

C. Ge 3p Spectra. The Ge 3p spectra for **1Ge** and **2Ge** are presented in Figure 9. Extraction of useful information from the germanium 3p edge was complicated by the low signal-to-background ratio at this edge (~125 eV), coupled with broad peak widths. Within the limits of the Ge 3p energy scale calibration (which is more challenging than normal on account of the absence of sharp features), little difference is observed between the unsaturated (**1Ge**) and saturated (**2Ge**) species. Although the Si 2p spectra of the silylenes[12] did show low-lying features reflecting the divalent character, these signals were extremely weak, consistent with a dominant 3p character to the relevant unoccupied energy levels and the fact that *n*p discrete excitation probes mainly the *n*s character of the unoccupied levels. The generally weak nature of discrete signals in *n*p core excitation spectra, coupled with the large background, is the reason there is little additional information obtainable from the Ge 3p edge. More useful information, complementing the carbene C 1s and silylene Si 1s[12] edges, could be acquired from the Ge 1s core excitation spectra. However, the spectroscopic information might be rather limited due to the large natural line width (>1 eV). The calculated Ge 1s spectrum has been presented in Figure 3. Also, comparison of Ge 3p signals of the Ge(II) and Ge(IV) species might be helpful in determining if the weak preedge features at ~123 eV in **1Ge** and **2Ge** are related to a b_2 LUMO. Attempts to synthesize the analogous tetravalent Ge compounds have so far been unsuccessful.

IV. Summary

An extensive set of core excitation spectra of divalent cyclodiammino species and related compounds have been presented and interpreted with the aid of high level ab initio core excitation calculations. These results, along with evidence from other techniques, have given considerable insight into the electronic structure and nature of bonding of **1** and **2**. The spectral and computational evidence points to a high degree of aromatic delocalization in the heterocyclic ring of **1C** and strong $N-E^{II}-N$ delocalization in all species. The most significant mode of stabilization of the divalent site is $N-E^{II}-N$ delocalization. This effect varies in strength as germylene < silylene < carbene, most likely reflecting the relative orbital overlap between the nitrogen centers and the empty p orbitals of the divalent site. The additional contribution from aromaticity would appear to be a factor in explaining the exceptional stability of the carbenes. The large energy shifts between analogous silylenes and carbenes and the qualitatively different unoccupied electronic structure in the carbenes relative to the silylenes or germylenes suggest that stabilization is quite sensitive to the radial extent of the valence orbitals. This may explain the difficulty of synthesizing the larger tin(II) and lead(II) analogues.

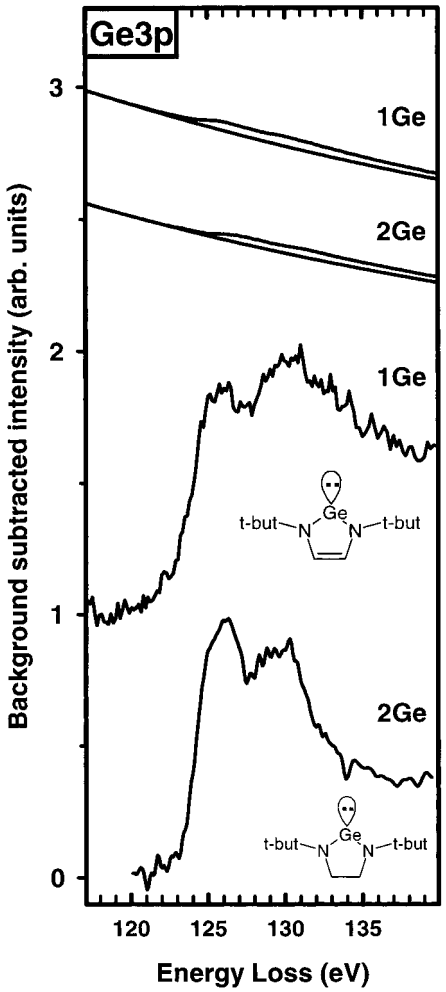

Figure 9. Ge 3p spectra of the unsaturated (**1Ge**) and saturated (**2Ge**) germylenes (bottom). The raw data and subtracted background are shown (top) to illustrate the "nonideal" conditions inherent to the germanium 3p edge. The vertical intensity scale, which refers to the background subtracted data only, is not on an absolute oscillator strength scale.

Acknowledgment. This work was supported financially by the Natural Sciences and Engineering Research Council of Canada. We thank Dr. N. Kosugi for providing the GSCF3 code and helpful comments with regard to its application in this project.

OM980882Z